Applied Geochemistry 97 (2018) 263–269

Contents lists available at ScienceDirect

Applied Geochemistry

journal homepage: www.elsevier.com/locate/apgeochem

Investigation of iron reduction by green tea polyphenols

M. Chrysochoou[a,*], J. Oakes[a], M.D. Dyar[b]

[a] Department of Civil and Environmental Engineering, University of Connecticut, Storrs, CT, 06269, USA
[b] Department of Astronomy, Mount Holyoke College, Holyoke, MA, USA

ARTICLE INFO

Editorial handling by Prof. M. Kersten

Keywords:
Iron nanoparticles
Green synthesis
Polyphenols
Green tea
Hexavalent chromium

ABSTRACT

The green synthesis of iron nanoparticles (Fe-NP) using plant extracts that are rich in polyphenols has become increasingly popular in recent years and a wide variety of plants have been used to this end. Although the reactivity of these Fe-NPs towards different contaminants has been shown, the exact composition of the nanoparticles remains controversial. Early studies claimed the formation of zero-valent iron, while others reported iron oxides such as magnetite and ferric oxyhydroxides and a variety of characterization techniques have been applied on solids recovered from the suspensions. This study reports on characterization conducted on original suspension produced from ferric iron reacted with three stoichiometries of green tea solution, utilizing X-ray Absorption Near Edge Structure (XANES) and Mössbauer spectroscopy. In addition, the suspensions were fractionated using nanofiltration and a host of techniques were applied to characterize the solid and the liquid fractions. Approximately 15% of the original Fe remained in solution, both as Fe(II) and Fe(III), while the remaining Fe formed nanoparticles that consist of primarily ferrous and ferric tannates, which have substantial reductive capacity for hexavalent chromium. Iron oxides were observed by Mössbauer spectroscopy only for the highest ratio of iron to green tea solution.

1. Introduction

The green synthesis of nanoparticles of iron (Fe-NP) and other metals (Ag, Au) using plant extracts has become increasingly popular in recent years (Herlekar et al., 2014; Nadagouda et al., 2014) and has been one of the key technologies for green and sustainable remediation (Virkutyte and Sharma, 2014), especially in light of their very low risk of ecotoxicity (Plachtova et al., 2018). The principle behind this technology is that the polyphenols contained in these extracts react with ferric iron (Fe(III)) to reduce it and produce zero-valent iron (Hoag et al., 2009). While the first studies employed green tea solution as the source of polyphenols (Hoag et al., 2009; Nadagouda et al., 2010), a wide variety of plant extracts have been utilized for the same purpose, including eucalyptus (Wang et al., 2014), sage (Wang et al., 2015), red wine and pomegranate juice (Mystrioti et al., 2016), blueberries (Manquian-Cerda et al., 2017), and twenty six different kinds of tree leaves (Machado et al., 2013a), to mention only a few of the available studies in the literature. Herlekar et al. (2014) provide a review of the relevant literature, which has continued to grow. Various authors have utilized the resulting suspensions to treat diverse contaminants and media, including domestic wastewater (Herlekar et al., 2014; Devatha et al., 2016), chlorinated solvents (Smuleac et al., 2011), hexavalent chromium (Chrysochoou et al., 2012; Fazlzadeh et al., 2017; Mystrioti et al., 2016), arsenic (Manquian-Cerda et al., 2017), nitrate (Wang et al. (2014a)) and ibuprofen-contaminated soils (Machado et al., 2013b).

While the reactivity of Fe-NP suspensions produced with green synthesis has been demonstrated through these treatability studies, the nature of the nanoparticles and the reaction pathways are less clear. Earlier studies utilized X-ray Diffraction (XRD) and transmission or scanning electron microscopy (TEM/SEM) to characterize the resulting nanoparticles and reported the presence of zero-valent iron (ZVI) (Hoag et al., 2009; Nadagouda et al., 2010). Njagi et al. (2011) and Machado et al. (2013a) failed to observe crystalline ZVI peaks in the XRD patterns and attributed this to the formation of an amorphous iron oxide shell around the nanoparticles upon drying. Mystrioti et al. (2016) utilized electron diffraction analysis in combination with TEM for Fe reacted with polyphenol-rich solutions and reported the presence zero-valent iron.

However, several other studies used a combination of techniques and reported the presence of iron oxide phases, specifically magnetite (Phumying et al., 2013; Singh et al., 2017), ferric oxide and oxyhydroxide (Shahwan et al., 2011), and mixtures thereof (Wang et al., 2014b, Herlekar et al., 2014). Markova et al. (2014) utilized Mössbauer spectroscopy and reported the presence of only Fe(II) and Fe(III)

* Corresponding author.
E-mail addresses: maria.chrysochoou@uconn.edu (M. Chrysochoou), mdyar@mtholyoke.edu (M.D. Dyar).

https://doi.org/10.1016/j.apgeochem.2018.08.026
Received 10 April 2018; Received in revised form 26 August 2018; Accepted 30 August 2018
Available online 31 August 2018
0883-2927/ © 2018 Elsevier Ltd. All rights reserved.

compounds; Machado et al. (2014) also found Fe(II) and Fe(III) using Mössbauer, but attributed the loss of ZVI to the sample preparation that induced oxidation.

This study focuses on the investigation of the composition and reactivity of Fe-NPs produced through a green tea synthesis, going beyond previous studies with two approaches: a) utilization of XANES spectroscopy directly on the suspension, avoiding any drying and sample preparation that could change the speciation of Fe; and, b) conducting fractionation tests with the use of nanofiltration and applying a suite of analytical and spectroscopic tests to the separated fractions, in order to obtain more detailed insight into the properties and reactivity of the Fe-NPs.

2. Materials and methods

2.1. Preparation of reagents

The green tea-iron suspension was prepared based on the method proposed in Hoag et al. (2009). Chunmee Special Grade #1 green tea (GT) leaves from Imperial Tea Garden were used in all experiments. The tea was prepared fresh daily and was brewed at 80 °C for 30 min. The leaves were pre-filtered using a Millipore prefilter (> 5 μm). The resulting filtrate was then vacuum filtered using a Millipore Durapore sterile, plain, white filter with a pore size of 0.22 μm. The average polyphenol concentration of this solution was determined to be 2.6 g/L gallic acid equivalents, using the Folin-Ciocalteu method (International Organization for Standardization (ISO) method 14502-1). The 0.1 M Fe solution was prepared using ferric chloride hexahydrate (ACS grade, Fisher Scientific). The two solutions were mixed together at room temperature at three volumetric ratios: one volume of green tea solution to two volumes of iron solution (1GT:2Fe) to form a solution with 66 mM total Fe, 2GT:1Fe to form 33 mM Fe, and 5GT:1Fe to form 16.7 mM Fe.

2.2. Experimental approach

The resulting suspension consists of suspended nanoparticles in an aqueous solution. To determine the speciation of Fe in the suspension, the experimental approach was adopted as illustrated in Fig. 1. The solid fraction was separated through nano-filtration in custom-built stainless steel dead-end cells. NF270 filter paper (pore size ~ 1 nm, molecular weight cutoff 340 Da) from Dow Water & Process Solutions was cut to fit the cell diameter using an X-ACTO knife and rinsed with DI water before being fit into the cell. A 10 mL aliquot of suspension was pipetted into the cell for each test. Nitrogen from a high-pressure tank flowed into the cell at 500 psi. The cell was positioned atop a stir plate and the outflow was captured in a plastic screw-cap vial. The filtration ran to completion and the filtrate was stored at 4 °C. The filter paper and solid mass were transported to a desiccator to dry under continuous flow of nitrogen gas. A variety of methods were employed in order to determine the type and concentrations of the iron species present in the two fractions, as described in the following sections.

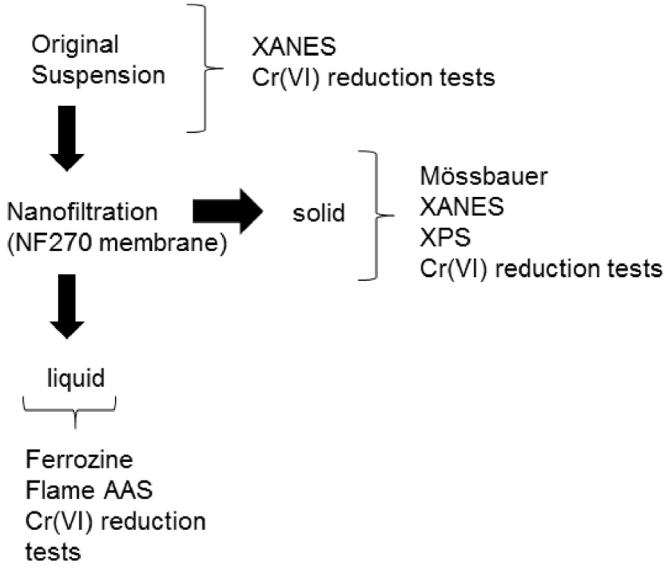

Fig. 1. Overview of experimental approach.

Finally, the reductive potential of the three fractions (suspension, solid, liquid) was evaluated using hexavalent chromium (Cr(VI)) as a probe compound. All tests were performed with 10 mL of original suspension as the reference amount of reactant, i.e. the solid and the liquid were recovered from the fractionation of 10 mL of original suspension using nano-filtration. The suspension and the solid filtrate were mixed with 200 mL of a 50 mg/L suspension, placed on a magnetic stirred for 24 h and then filtered and residual Cr(VI) was measured with EPA method 7196a. The pH of the batch reduction tests was adjusted to ~3 if necessary using concentrated HNO_3 to run the reaction to completion without H^+ being a limiting factor and to prevent rapid oxidation of Fe(II) in solution or suspension. For liquid experiments, it was found that the reductive capacity was too low to accurately measure with this method, so that the volume was reduced to 50 mL of 50 mg/L stock solution for 10 mL of suspension to obtain accurate readings of the final Cr(VI) concentration.

2.3. Analytical and spectroscopic methods

For Fe(II) analysis in solution, the revised ferrozine method by Viollier et al. (2000) allows for the determination of Fe(II) in the presence of Fe(III) in solution and the details are provided in Supplementary Information. For total Fe analysis, flame Atomic Absorption Spectroscopy AAS (Thermo Scientific Niton iCE 3000) was employed according to EPA method 7000B, including blanks, standards and duplicates for quality assurance-quality control. All Fe-GT ratios were tested in five replicates, for which averages and standard deviations are given.

XPS analysis was carried out using a PHI Multiprobe with an aluminum anode. The full survey spectra were collected using a pass energy of 100 eV and a scan rate of 1eV per step. High resolution spectra were collected at a pass energy of 50 eV and a scan rate of 0.1 eV per step. High resolution scans were performed on carbon, oxygen, and iron peaks. The spectra were analyzed using the CasaXPS software. Binding energy data was derived from the spectra fitting using the adventitious carbon C1s peak at 284.8 eV (Grosvenor et al., 2004). Shirley background curves were used for all fittings and specifically for Fe, separate background curves were fitted to the $^2p_{3/2}$ and $^2p_{1/2}$ peaks. The full-width at half maximum for peak fitting was constrained to equal values for all peaks within a fit, and the peak areas for the $^2p_{1/2}$ peaks were constrained to half the areas of the $^2p_{3/2}$ peaks.

XANES analysis was performed on beamline X23A2 operated by the National Institute of Standards and Technology, at the National Synchrotron Light Source (Brookhaven National Laboratory, Upton, NY). Incident X-ray energy was scanned across the XANES region (100 eV below the edge up to 400 eV above the edge) of the Fe K-edge (E = 7112 eV) using a Si(311) monochromator and a single-bounce harmonic rejection mirror. The monochromator was calibrated using a Fe foil. Fluorescent X-rays were collected using a Stern-Heald fluorescence detector. Samples of the GT-Fe suspensions were pipetted into a sample holder between two layers of Kapton tape for analysis. Final spectra are the result of a single scan; this was preferred because evaluation of sequential scans showed beam damage, i.e. progressive oxidation of the Fe in the sample. XANES data were processed using the Athena software (Ravel and Newville, 2005), including normalization, calibration and alignment.

Mössbauer sample mounts were made from these dried products by

mixing ~40 mg of sample with sugar in a diamonite mortar and pestle and then gently heaping the mixture into plastic washers and confined with Kapton tape. Mössbauer measurements were taken at 295K, on a Web Research Co. (now See Co.) W100 spectrometer using a ~10 mCi ^{57}Co source in rhodium. Run times ranged from 24 to 48 h. Spectra were collected in 2048 channels and then all spectral baselines were corrected for the Compton scattering of 122 keV gamma rays by electrons inside the detector. The corrected data are equal to A/(1-b), where A is the counts of the uncorrected absorption and b is the Compton fraction determined through recording the counts with and without a 14.4 keV stop filter (~2 mm Al foil) in the gamma ray beam. While this correction does not change the results of the fits, it does allow for accurate determination of the % absorption in each spectrum. Each spectrum was then folded and corrected for nonlinearity in WMOSS. Interpolation to a linear-velocity scale was accomplished by using the room temperature spectrum of 25 μm α-Fe foil as a calibration standard.

Samples were fit using the Mex_field program, which solves the full hyperfine interaction Hamiltonian for multiple distributions modeled by Lorentzian lines, and minimizes the chi squared deviation between the fitted and experimental spectrum using center shift, quadrupole shift, full width at half maximum, hyperfine field, and distribution area as free parameters (Vandenberghe et al., 2001). More details of these Mössbauer parameters are described by Dyar et al. (2006). All isomer shifts are given referred to α-Fe. All samples were run at 295K using a 4 mm/s velocity scale, and most were also run at 140K, 80K, and 4K using a 12 mm/s scale.

3. Results and discussion

3.1. Liquid fraction analyses

Fig. 2 shows the average values for Fe(II) measured by the ferrozine method, total Fe in the liquid measured by FLAAS and Fe(III) calculated as the difference between the two for individual measurements. The Fe available in solution for the three mixing ratios was 17–20% for 2GT:1Fe and 1GT:2Fe, and 11% for 5GT:1Fe compared to the totally available Fe. Thus, the majority of the initially dissolved Fe precipitated upon contact with the green tea solution. The final pH of the 2GT:1Fe and 1GT:2Fe was 1.6 and the 5GT:1Fe was 2.0. As shown in Fig. 2, this

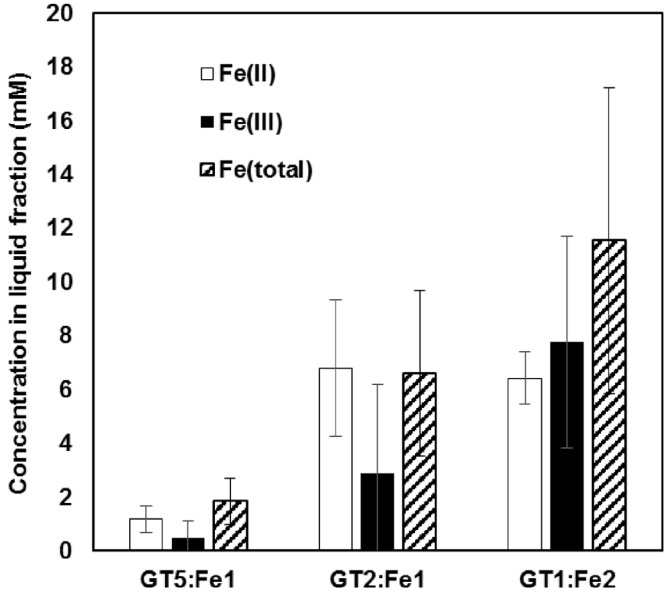

Fig. 2. Average values of five replicates for dissolved Fe species in liquid fraction of GT-Fe suspensions (Fe(III) = Fe (tot)-Fe(II) for individual measurements).

low pH is due to the presence of unhydrolyzed Fe(III) in solution. According to a simple geochemical model (Visual Minteq, Gustafsson, 2011), a solution with dissolved Fe(III) and Cl^- has an equilibrium pH that changes logarithmically with the Fe^{3+} concentration; 10 mM Fe (III) results in pH 1.6, and 10^{-3} Fe^{3+} to pH 5.6 (Fig. S1). The precipitation of various Fe-bearing phases results in solubility control that ultimately influences equilibrium pH as well. The pH of nZVI solutions is typically around 9, due to the formation of $Fe(OH)_2$(s) and/or Fe_3O_4(s), both of which have an approximate equilibrium pH of 9 (Reardon, 2005). As shown in Fig. S1, the pH of the three suspensions approximately followed the logarithmic trend, confirming the assumption that pH is controlled by the free Fe^{3+} in solution, despite the presence of dissolved Fe^{2+} and solid precipitates.

In term of the reaction efficiency, we can evaluate the reductive potential of the green tea by making certain simplifications. Previous work has shown that Fe(III) to Fe(II) reduction by polyphenols depends on the molar ratio of the polyphenols to the total iron concentration. Low molecular weight (MW) compounds such as catechol produce 1 or 2 mol of Fe per mol of compound, while high MW weight compounds such as epigallocatechin gallate (EGCG) produce 1–4 mol of Fe per mol depending on the Fe-to-compound ratio (Hynes and Coinceanainn, 2001; Ryan and Hynes, 2007). Specifically, a Fe:EGCG ratio of 4:1 was observed to produce 4 moles of Fe^{2+}, 3:1 produced 3 mol and 1:1 produced 1 mol (Ryan and Hynes, 2007). Thus, an excess of polyphenols does not necessarily result in more reduction.

In this study, the polyphenol content in the green tea solution was measured at an average of 2.6 g GAE/L using the Folin-Ciocalteu method, which is equal to 15.3 mmol [PH]/L using the gallic acid MW of 170 g/L. As a simplification, we will assume that 30% of this content behaves as a high MW compound (EGCG), and the remaining as low MW (catechin), which is consistent with analysis of various green tea solutions (Table S1, Henning et al., 2003). The initial polyphenol content of the suspension may be calculated on the basis of the GT:Fe ratio. Using the molar ratio and total concentrations of each group of compounds, we may calculate theoretical yields of Fe(II) in solution (Table 1). The 5GT:1Fe suspension has a Fe:PH molar ratio below 2 and will behave in the same way for low and high MW compounds, producing a maximum of 1 mol Fe(II) per mol of polyphenol. The suspension 2GT:1Fe has a molar ratio Fe:PH exceeding 3; in this case, 33% will behave as high MW producing 3 mols of Fe and the remaining as low MW, producing 2 mols of Fe. This solution will theoretically produce the maximum Fe(II), because it has a high Fe:PH ratio and a relatively high total polyphenol concentration as well. Indeed, the 2GT:1Fe suspension produced the highest concentrations of Fe(II) in the liquid fraction. It is also apparent from this analysis that excess Fe(III) will remain unreacted and the 2Fe:1GT will have the largest excess of Fe(III). The measured values for both Fe(II) and Fe(III) in solution are much lower than the theoretical potential, which is expected given that both are removed by precipitation. Thus, knowledge of Fe speciation in the solid is also required to conduct further assessment of the suspensions and their reductive potential.

3.2. Spectroscopic analyses of solid and suspension

3.2.1. Mössbauer spectroscopy

The Mössbauer spectra for the five experimental conditions (295 K at 4 mm/s and four temperatures (295, 140, 80 and 4 K) at ± 12 mm/s are shown in Fig. S2, while Table 2 summarizes the resulting parameters for the 295 K, ± 4 mm/s spectra. The lower-resolution (± 12 mm/s) spectra at different temperatures are utilized to determine the presence of iron oxides that emerge as sextets at lower temperatures, while the higher resolution ± 4 mm/s spectra at 295 K are used to investigate the presence of Fe(II) at low amounts. As seen in Fig. S2, the only sample that showed the presence of Fe(III), identified as akaganeite (β-FeOOH), was 2Fe:1GT. Parameters of its two sextets at 4 K were IS = 0.51 and 0.48 mm/s, QS = −0.53 and −0.19 mm/s, and

Table 1
Theoretical calculations for Fe^{2+} production potential in the three suspensions.

GT:Fe	[PH] mmol/L	[Fe] mmol/L	Fe:PH Molar Ratio	Theoretical mmol/L of total Fe^{2+} produced	Average Actual mmol/L of Fe^{2+} in Liquid Fraction	Theoretical unreacted Fe^{3+} (mM)	Average Actual mmol/L of Fe^{3+} in Liquid Fraction
5	12.8	16.7	1.3	12.8	1.2	3.9	0.5
2	10.2	33.3	3.3	20.4	6.8	9.5	2.9
1/2	5.1	66.6	13.1	15.4	6.4	53	7.8

Table 2
Mössbauer parameters of samples at 295 K and ± 4 mm/s.

	sample	1GT:2Fe	2GT:1Fe	5GT:1Fe
Ferric 1	IS		0.26	0.21
	QS		0.71	0.42
	Width		0.49	0.51
	Area		26	24
Ferric 2	IS	0.35	0.43	0.44
CI complex	QS	0.70	0.63	0.56
	Width	0.55	0.42	0.30[a]
	Area	69	69	24
Ferric 3	IS	0.57		0.45
CII complex	QS	0.70		0.90
	Width	0.40[a]		0.300[a]
	Area	15		53
Ferrous 1	IS	1.18	1.18	
	QS	1.61	1.90	
	Width	0.33		
	Area	6	3	
Ferrous 2	IS	1.27	1.15	
	QS	2.18	2.66	
	Width	0.23[a]	0.23[a]	
	Area	5	2	
Ferrous 3	IS	1.24		
	QS	2.88		
	Width	0.23[a]		
	Area	4		
	X^2	533.07	497.96	596.13
	$\|X^2\|$	1.04	0.97	1.16
	% ferrous	16	5	0

[a] Parameter fixed.

a hyperfine field of 45.35 and 48.66 T. The remaining two samples showed no evidence of oxides and no presence of zero-valent iron; thus, the remaining candidates to account for the observed spectra are organic Fe-complexes.

Literature evidence supports this conclusion. Several studies have investigated the interaction between tannins, polyphenols of high MW (> 500 kDa), and iron forms found in steel corrosion (Gust and Suwalski, 1994, Jaen et al., 2003, 2011). Jaen et al. (2003) observed that tannin concentrations above 1% inhibited the formation of iron oxides upon interaction of a $Fe(NO)_3$ solution with tannins. Both Gust and Suwalski (1994) and Jaen et al. (2011) utilized Mössbauer spectroscopy and reported the formation of two ferric and one ferrous tannate precipitates. Ferric tannates were reported as CI and CII, which were presumed analogous to the dissolved complexes with a single and two polyphenol ligands (Fig. S3). The Mössbauer parameters for these two complexes at 300 K are QS 0.80 ± 0.06 mm/s and IS 0.43 ± 0.02 mm/s for CI and QS 1.19 ± 0.08 mm/s and IS 0.44 ± 0.02 mm/s for CII (Gust and Suwalski, 1994). Jaen et al. (2011) reported slightly lower QS values around 0.6–0.7 mm/s for the CI complex. Thus, the complex identified as Ferric 2 in Table 2 is potentially analogous to the CI complex in these studies, while Ferric 3 could be analogous to the CII complex.

Fe(II) precipitates were identified in two room temperature spectra, 1GT:2Fe and 2GT:1Fe and their relative percentage on the basis of the observed areas were 16% and 5%, respectively. It should be noted that the required sample drying for sample preparation is likely to result in partial oxidation of Fe(II), despite the precaution of nitrogen purging. In both cases, the observed precipitate is not an oxide, similar to the Fe (III) ones, thus an organically-complexed precipitate is the most likely candidate for this Fe species as well.

Thus, the main unequivocal conclusion of the Mössbauer analysis is that Fe oxide formation is not substantial, with the exception of the 1GT:2Fe sample with the highest Fe content. Based on the amount of polyphenols measured as gallic acid equivalents (GAE), there is not enough concentration of polyphenols to account for the organic complexation of all Fe that remains in the solid. Thus, the presence of other organic Fe complexes that are not tannates is necessary to close the mass balance. This conclusion will inform the results of the remaining spectroscopic analyses as well.

3.2.2. XANES spectroscopy

The redox states of Fe in the suspension and the solid samples recovered through nanofiltration were evaluated by examining both the normalized spectrum and the first derivative (Fig. 3), using reference values and spectra by O'Day et al. (2004). The pre-edge peak (first peak in derivatives) centroid was located at 7113.5–7114 eV for all spectra, which is associated with higher oxidation states, specifically Fe(III). It should be noted here that some variability in these values is expected; for example, Prietzel et al. (2007) reported reference values for the pre-edge peak at least 1 eV higher compared to O'Day et al. (2004), even though both studies reported using Fe foil and 7112 eV as standard for energy calibration. Regardless of this fluctuation, the observed values for the pre-edge peak are too high to correspond to Fe (0) and more likely to account for a Fe(III) species. In terms of the post-edge spectrum, it resembles most closely the spectrum of Fe(III)-citrate shown by O'Day et al. (2004), which was also the only spectrum with a single post-edge peak in the first derivative. Thus, the XANES analysis indicates that the predominant phase in both the suspension and the dry solid is a Fe(III)-organic complex. This agrees with the observations of the Mössbauer analysis. No substantial differences were observed between the samples with different Fe:GT ratios.

3.2.3. XPS results

High resolution scans were obtained in two energy regions: one for carbon (280–300 eV) to conduct energy calibration (Fig. S4 and Table S2) and for iron species (700–740 eV) (Fig. S5). There were two major challenges in performing the spectral analysis: calibration of the spectrum based on the graphite peak was difficult because of the overlap with the carbon energies in the polyphenol groups; and, iron peaks were very small because of the low amount retained in the solid compared to the amount of organic matter.

Energy calibration using the carbon peak is performed on the basis of the adventitious C1s peak with a fixed energy at 284.8 eV (Grosvenor et al., 2004). In this case, the precipitated organics contributed additional intensity, so that the observed carbon peak was quite broad and centered at substantially higher energies, between 288 and 292 eV, with peak broadening increasing with the green tea dosage. This energy range is typical for carbon associated with oxygen bonds, including carbonate and carboxylic groups, as indicated by a survey of the XPS NIST database. Akhavan et al. (2012) studied the reduction of graphene oxide by green tea polyphenols in the presence of iron and the C1s XPS spectra showed peaks at 285 eV (C-C, C = C and C-H bonds) and higher peaks at 286.7, 287.4, 288.3, and 289.4 eV that were attributed to the

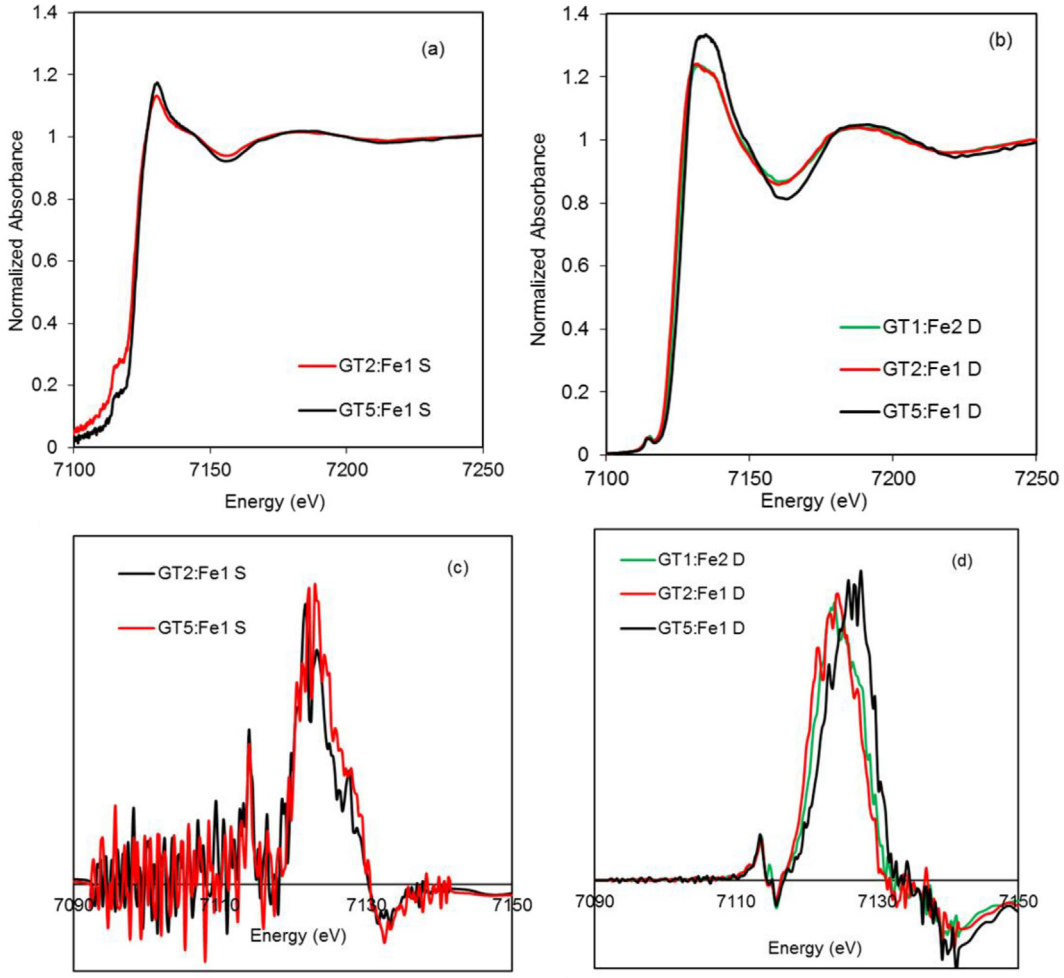

Fig. 3. Normalized (a, b) and first-derivative (c, d) XANES spectra of GT-Fe suspensions (a,c) and GT-Fe samples after nanofiltration (b,d).

C-OH, C-O-C, C-O, and O-C-OH oxygen-containing functional groups, respectively. Peak fitting in all three spectra lead to energies consistent with the above values (Table S1) as well as peaks related to CO_2 presence. The lower-energy peak around 285 eV was used to conduct energy calibration for Fe and this was done with reference to 284.8 eV.

As seen in Table 3, the Fe $^2p_{3/2}$ and $^2p_{1/2}$ peaks for Fe were all observed at considerably higher binding energies compared to typical Fe(III) species, e.g. 710.8 eV for goethite and 711.2 eV for hematite (Baltrusaitis et al., 2007). Fe(II) oxides have even lower energies around 707–709 eV and zero-valent iron has a binding energy of 706.5–706.9 eV, according to the National Institute of Standards and Technology (NIST) XPS database that includes a wide range of references (NIST, 2012). Higher energies for Fe compounds are typically associated with phosphates and sulfates (e.g., Wang and Sherwood, 2002, Eggleston et al., 1996) and with adsorbed species such as sulfate (Baltrusaitis et al., 2007). In general, an increase in binding energy of Fe compounds is associated with a reduction in symmetry (Grosvenor et al., 2004) and so it is considered likely that the observed peaks are associated with Fe(III)-compounds with adsorbed or complexed with organic compounds. Another possibility is that the energy calibration is erroneous and that the highest peak should be used for energy correction. Even if that were the case, the maximum shift in the observed peaks would be 3 eV, which would bring the binding energies of the $^2p_{3/2}$ peak down to 710–711 eV. These would still be Fe(III) and Fe(II) species, and ZVI could not be present. The progressive reduction in binding energy with increased green tea dosage points to increased reduction or complexation of Fe, which agrees with the chemical analysis data.

Previous XPS studies of iron reduced by different types of extracts have reported the presence of iron oxides. Specifically, Weng et al. (2016) reported the identification of ferric oxide by the peak at 710.8 eV, and Guo et al. (2017) reported ferric oxide at 711.05 eV and ferrous oxide at 708.6 eV. In both studies the use of the C1s peak for calibration was mentioned, however the issue of multiple carbon peaks at higher energy due to the organic extracts were not discussed and thus the accuracy of the calibration remains unclear.

Table 3
Summary of observed and theoretical Fe peaks in energy-calibrated XPS spectra.

	Fe $^2p_{3/2}$	Satellite	Fe $^2p_{1/2}$	Satellite
1GT:2Fe	714.37	n/a	727.88	733.89
2GT:1Fe	713.07	716.14	726.57	731.27
5GT:1Fe	712.95	716.48	726.67	730.98

3.3. Cr(VI) reduction experiments

Fig. 4 shows the results of the Cr(VI) reduction experiments for the liquid, solid and suspensions. The results indicate that there is good agreement between the amount of Cr(VI) reduced by the green tea solution and the sum of the two fractions obtained by nanofiltration. Nanofiltration involves the separation of large organic molecules and other compounds through mechanisms of size exclusion and adsorption. López-Muñoz et al. (2009) determined a molecular weight cut-off (MWCO) of 340 for the NF 270 membrane used in this study, which

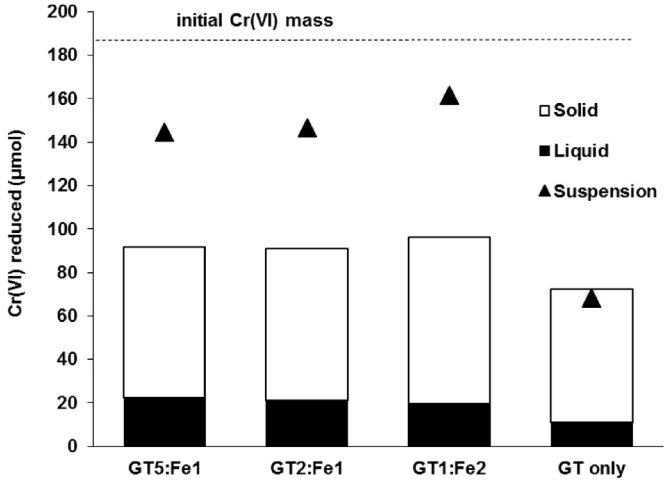

Fig. 4. Reductive capacity of liquid and solid fractions compared to suspension for the three Fe:GT dosages.

corresponds to the MW weight of a compound retained with 90% efficiency by the membrane. López-Muñoz et al. (2009) developed the retention curve using polyethylene glycol compounds, which are uncharged and should not exhibit significant adsorption (López-Muñoz et al., 2009). Polyphenols should also be uncharged at pH 3, given that the pK_as of most polyphenol compounds are in the neutral-to-alkaline region. Thus, we adopted the retention curve to assess polyphenol retention by the NF270 membrane, considering the composition provided by Henning et al. (2003) (Table S1). The majority of the polyphenols should be retained by the membrane, while only ~15% of EGCG may pass through the membrane, and about 35–40% of caffeine and gallic acid. Cr(VI) can be reduced by caffeic acid (Deiana et al., 2007), so that it is very likely that caffeine and gallic acid are Cr(VI) reductants as well. Based on the retention curve and using the average molar fractions of Table S2, it follows that only 17% of the original mass of polyphenols is present in the liquid fraction, i.e. the fraction that goes through the NF270 membrane. Fig. 4 indicates that this fraction possesses only 15% of the total reductive capacity of the original green tea solution and thus the two analyses are in good agreement.

In contrast to green tea alone, there is poor agreement when comparing the reductive capacity of the GT-Fe suspensions and the sum of the respective solid and liquid fractions. Specifically, the additive reductive capacity is ~60% of the suspension reductive capacity for all three formulations. It is probable that the iron present on the filter loses its reductive capacity during the filtration process. This loss may be due to multiple processes, such as oxidation and agglomeration of the formed nanoparticles. It is also possible that the continuous presence of green tea in solution may lead to regeneration of Fe(II) after reaction with Cr(VI), further enhancing the reaction, which cannot occur as easily in the solid phase. However, the reductive capacity of the filtered solid remains high (72–77 µmol per 5 mL of all three formulations), which indicates that regeneration may still be possible in the wet filtered solid as well.

Interestingly, there were very small differences in the performance of the three mixes and in fact the 1GT:2Fe mixture outperformed the others. There are several processes to decouple in order to explain these results, namely:

- The mass of initially available polyphenols decreases with increasing Fe.
- The mass of polyphenols reacting with the added Fe(III) increases with increasing Fe. It is not trivial to assess the available concentration remaining in the GT-Fe suspension that can further reduce either Cr(VI) or Fe(III) resulting from the Cr(VI)-Fe(II) reaction.
- The mass and reactivity of polyphenols that are retained in the solid vs. pass in the liquid fraction are also likely different in the three mixes. The organic molecules in the liquid of green tea alone are not the same as in the liquid of the filtered GT-Fe suspension.

Answering these questions requires more detailed investigation with regard to the reactions of specific polyphenols that are beyond the scope of this study.

4. Conclusions

The characterization of three ratios of GT:Fe mixtures showed that approximately 15% of the initially available Fe remains pure dissolved upon reaction with the green tea. Both Fe(II) and Fe(III) are present in solution and the 2GT:1Fe ratio produced the majority of Fe(II) (~66% of the total dissolved Fe). The presence of dissolved, unhydrolyzed Fe (III) in solution is related to the substantial residual acidity in all three GT:Fe suspensions, all of which had a pH of 2 or lower.

The remaining Fe precipitated in the form of what seems to be primarily ferrous and ferric organic phases, such as tannates. Mössbauer spectroscopy showed that no oxides were present in the solid, except in the case of the 1GT:2Fe ratio with the most iron, which had akaganeite as a major phase. XANES spectroscopy conducted on the original suspensions also showed that no zero-valent iron was present and the organically-complexed ferric iron is the primary species in suspension. All three formulations had more than double the reductive capacity for Cr(VI) at pH 3 compared to the green tea alone, albeit with small differences between them. The 1GT:2Fe mix with the most iron outperformed the other two formulations. Comparison of the suspension performance with the solid and liquid fractions showed that the suspension reduction capacity exceeded the sum of the individual fractions, and that the solid fraction was primarily responsible for the reductive potential. Combined, this indicates that the suspension possesses a regenerative capacity for ferrous iron production.

Acknowledgments

The authors wish to thank Dr. Jeff McCutcheon and Liwei Huang for providing access to the nanofiltration set up and assisting with experiments, and Elizabeth Sklute for assistance with the Mössbauer fits.

Appendix A. Supplementary data

Supplementary data related to this article can be found at https://doi.org/10.1016/j.apgeochem.2018.08.026.

References

Akhavan, O., Kalaee, M., Alavi, Z.S., Ghiasi, S.M.A., Esfandiar, A., 2012. Increasing the antioxidant activity of green tea polyphenols in the presence of iron for the reduction of graphene oxide. Carbon 50, 3015–3025. https://doi.org/10.1016/j.carbon.2012.02.087.

Baltrusaitis, J., Cwiertny, D.M., Grassian, V.H., 2007. Adsorption of sulfur dioxide on hematite and goethite particle surfaces. Phys. Chem. Chem. Phys. 9, 5542–5554. https://doi.org/10.1039/B709167B.

Chrysochoou, M., Johnston, C.P., Dahal, G., 2012. A comparative evaluation of hexavalent chromium treatment in contaminated soil by calcium polysulfide and green-tea nanoscale zero-valent iron. J. Hazard Mater. 201, 33–42. https://doi.org/10.1016/j.jhazmat.2011.11.003.

Deiana, S., Premoli, A., Senette, C., 2007. Reduction of Cr(VI) by caffeic acid. Chemosphere 67, 1919–1926. https://doi.org/10.1016/j.chemosphere.2006.12.003.

Devatha, C.P., Thalla, A.K., Katte, S.Y., 2016. Green synthesis of iron nanoparticles using different leaf extracts for treatment of domestic waste water. J. Clean. Prod. 139, 1425–1435. https://doi.org/10.1016/j.jclepro.2016.09.019.

Dyar, M.D., Agresti, D.G., Schaefer, M.W., Grant, C.A., Sklute, E.C., 2006. Mössbauer spectroscopy of Earth and planetary materials. Annu. Rev. Earth Planet Sci. 34, 83–125. https://doi.org/10.1146/annurev.earth.34.031405.125049.

Eggleston, C.M., Ehrhardt, J.-J., Stumm, W., 1996. Surface structural controls on pyrite oxidation kinetics: an XPS-UPS, STM, and modeling study. Am. Mineral. 81, 1036–1056. https://doi.org/10.2138/am-1996-9-1002.

Fazlzadeh, M., Rahmani, K., Zarei, A., Abdoallahzadeh, H., Nasiri, F., Khosravi, R., 2017.

A novel green synthesis of zero valent iron nanoparticles (NZVI) using three plant extracts and their efficient application for removal of Cr(VI) from aqueous solutions. Adv. Powder Technol. 28, 122–130. https://doi.org/10.1016/j.apt.2016.09.003.
Grosvenor, A.P., Kobe, B.A., Biesinger, M.C., McIntyre, N.S., 2004. Investigation of multiplet splitting of Fe 2p XPS spectra and bonding in iron compounds. Surf. Interface Anal. 36, 1564–1574. https://doi.org/10.1002/sia.1984.
Guo, M., Weng, X., Wang, T., Chen, Z., 2017. Biosynthesized iron-based nanoparticles used as a heterogeneous catalyst for the removal of 2,4-dichlorophenol. Separ. Purif. Technol. 175, 222–228. https://doi.org/10.1016/j.seppur.2016.11.042.
Gust, J., Suwalski, J., 1994. Use of mössbauer spectroscopy to study reaction products of polyphenols and iron compounds. Corrosion 50, 355–365. https://doi.org/10.5006/1.3294344.
Gustafsson, J.P., 2011. Visual MINTEQ Ver. 3.0. Department of Land and Water Resources Engineering, Royal Institute of Technology, Stokholm, Sweden.
Henning, S.M., Fajardo-Lira, C., Lee, H.W., Youssefian, A.A., Go, V.L.W., Heber, D., 2003. Catechin content of 18 teas and a green tea extract supplement correlates with the antioxidant capacity. Nutr. Canc. 45, 226–235. https://doi.org/10.1207/S15327914NC4502_13.
Herlekar, M., Barve, S., Kumar, R., 2014. Plant-mediated green synthesis of iron nanoparticles [WWW Document]. Journal of Nanoparticles. https://doi.org/10.1155/2014/140614.
Hoag, G.E., Collins, J.B., Holcomb, J.L., Hoag, J.R., Nadagouda, M.N., Varma, R.S., 2009. Degradation of bromothymol blue by 'greener' nano-scale zero-valent iron synthesized using tea polyphenols. J. Mater. Chem. 19, 8671–8677. https://doi.org/10.1039/B909148C.
Hynes, M.J., Ó Coinceanainn, M., 2001. The kinetics and mechanisms of the reaction of iron(III) with gallic acid, gallic acid methyl ester and catechin. J. Inorg. Biochem. 85, 131–142. https://doi.org/10.1016/S0162-0134(01)00205-7.
Jaén, J.A., Araúz, E.Y., Iglesias, J., Delgado, Y., 2003. Reactivity of tannic acid with common corrosion products and its influence on the hydrolysis of iron in alkaline solutions. Hyperfine Interact. 148–149, 199–209. https://doi.org/10.1023/B:HYPE.0000003781.45888.28.
Jaén, J.A., Obaldía, J.D., Rodríguez, M.V., 2011. Application of Mössbauer spectroscopy to the study of tannins inhibition of iron and steel corrosion. Hyperfine Interact. 202, 25–38. https://doi.org/10.1007/s10751-011-0337-1.
López-Muñoz, M.J., Sotto, A., Arsuaga, J.M., Van der Bruggen, B., 2009. Influence of membrane, solute and solution properties on the retention of phenolic compounds in aqueous solution by nanofiltration membranes. Separ. Purif. Technol. 66, 194–201. https://doi.org/10.1016/j.seppur.2008.11.001.
Machado, S., Grosso, J.P., Nouws, H.P.A., Albergaria, J.T., Delerue-Matos, C., 2014. Utilization of food industry wastes for the production of zero-valent iron nanoparticles. Sci. Total Environ. 496, 233–240. https://doi.org/10.1016/j.scitotenv.2014.07.058.
Machado, S., Pinto, S.L., Grosso, J.P., Nouws, H.P.A., Albergaria, J.T., Delerue-Matos, C., 2013a. Green production of zero-valent iron nanoparticles using tree leaf extracts. Sci. Total Environ. 445, 1–8. https://doi.org/10.1016/j.scitotenv.2012.12.033.
Machado, S., Stawiński, W., Slonina, P., Pinto, A.R., Grosso, J.P., Nouws, H.P.A., Albergaria, J.T., Delerue-Matos, C., 2013b. Application of green zero-valent iron nanoparticles to the remediation of soils contaminated with ibuprofen. Sci. Total Environ. 461, 323–329. https://doi.org/10.1016/j.scitotenv.2013.05.016.
Manquián-Cerda, K., Cruces, E., Angélica Rubio, M., Reyes, C., Arancibia-Miranda, N., 2017. Preparation of nanoscale iron (oxide, oxyhydroxides and zero-valent) particles derived from blueberries: reactivity, characterization and removal mechanism of arsenate. Ecotoxicol. Environ. Saf. 145, 69–77. https://doi.org/10.1016/j.ecoenv.2017.07.004.
Markova, Z., Novak, P., Kaslik, J., Plachtova, P., Brazdova, M., Jancula, D., Siskova, K.M., Machala, L., Marsalek, B., Zboril, R., Varma, R., 2014. Iron(II,III)–Polyphenol complex nanoparticles derived from green tea with remarkable ecotoxicological impact. ACS Sustain. Chem. Eng. 2, 1674–1680. https://doi.org/10.1021/sc5001435.
Mystrioti, C., Xanthopoulou, T.D., Tsakiridis, P., Papassiopi, N., Xenidis, A., 2016. Comparative evaluation of five plant extracts and juices for nanoiron synthesis and application for hexavalent chromium reduction. Sci. Total Environ. 539, 105–113. https://doi.org/10.1016/j.scitotenv.2015.08.091.
Nadagouda, M., Iyanna, N., Lalley, J., Han, C., Dionysiou, D., Varma, R., 2014. Synthesis of silver and gold nanoparticles using antioxidants from blackberry, blueberry, pomegranate, and turmeric extracts. ACS Sustain. Chem. Eng. 2 (7), 1717–1723.
Nadagouda, M.B., Castle, A.C., Murdock, R.M., Hussain, S.S., Varma, R., 2010. In vitro biocompatibility of nanoscale zerovalent iron particles (NZVI) synthesized using tea polyphenols. Green Chem. 12, 114–122. https://doi.org/10.1039/B921203P.
NIST (National Institute of Standards and Technology), 2012. NIST X-ray Photoelectron Spectroscopy Database, NIST Standard Reference Database 20. Version 4.1, URL. https://srdata.nist.gov/xps/Default.aspx, Accessed date: 18 July 2017.
Njagi, E.C., Huang, H., Stafford, L., Genuino, H., Galindo, H.M., Collins, J.B., Hoag, G.E., Suib, S.L., 2011. Biosynthesis of iron and silver nanoparticles at room temperature using aqueous sorghum bran extracts. Langmuir 27, 264–271. https://doi.org/10.1021/la103190n.
O'Day, P.A., Rivera, N., Root, R., Carroll, S.A., 2004. X-ray absorption spectroscopic study of Fe reference compounds for the analysis of natural sediments. Am. Mineral. 89, 572–585. https://doi.org/10.2138/am-2004-0412.
Phumying, S., Labuayai, S., Thomas, C., Amornkitbamrung, V., Swatsitang, E., Maensiri, S., 2013. Aloe vera plant-extracted solution hydrothermal synthesis and magnetic properties of magnetite (Fe3O4) nanoparticles. Appl. Phys. A 111, 1187–1193. https://doi.org/10.1007/s00339-012-7340-5.
Plachtová, P., Medříková, Zdenka, Zbořil, Radek, Tuček, Jiří, Varma, Rajender S., Maršálek, Blahoslav, 2018. Iron and iron oxide nanoparticles synthesized with green tea extract: differences in ecotoxicological profile and ability to degrade malachite green. ACS Sustain. Chem. Eng. 6 (7), 8679–8687.
Prietzel, J., Thieme, J., Eusterhues, K., Eichert, D., 2007. Iron speciation in soils and soil aggregates by synchrotron-based X-ray microspectroscopy (XANES,μ-XANES). Eur. J. Soil Sci. 58, 1027–1041. https://doi.org/10.1111/j.1365-2389.2006.00882.x.
Ravel, B., Newville, M., 2005. ATHENA, ARTEMIS, HEPHAESTUS: data analysis for X-ray absorption spectroscopy using IFEFFIT. J Synchrotron Rad, J Synchrotron Radiat 12, 537–541. https://doi.org/10.1107/S0909049505012719.
Reardon, E.J., 2005. Zerovalent irons: styles of corrosion and inorganic control on hydrogen pressure buildup. Environ. Sci. Technol. 39, 7311–7317. https://doi.org/10.1021/es050507f.
Ryan, P., Hynes, M.J., 2007. The kinetics and mechanisms of the complex formation and antioxidant behaviour of the polyphenols EGCg and ECG with iron(III). J. Inorg. Biochem. 101, 585–593. https://doi.org/10.1016/j.jinorgbio.2006.12.001.
Shahwan, T., Abu Sirriah, S., Nairat, M., Boyacı, E., Eroğlu, A.E., Scott, T.B., Hallam, K.R., 2011. Green synthesis of iron nanoparticles and their application as a Fenton-like catalyst for the degradation of aqueous cationic and anionic dyes. Chem. Eng. J. 172, 258–266. https://doi.org/10.1016/j.cej.2011.05.103.
Singh, K.K., Senapati, K.K., Sarma, K.C., 2017. Synthesis of superparamagnetic Fe3O4 nanoparticles coated with green tea polyphenols and their use for removal of dye pollutant from aqueous solution. Journal of Environmental Chemical Engineering 5, 2214–2221. https://doi.org/10.1016/j.jece.2017.04.022.
Smuleac, V., Varma, R., Sikdar, S., Bhattacharyya, D., 2011. Green synthesis of Fe and Fe/Pd bimetallic nanoparticles in membranes for reductive degradation of chlorinated organics. J. Membr. Sci. 379, 131–137. https://doi.org/10.1016/j.memsci.2011.05.054.
Vandenberghe, R.E., San, E.V., Grave, E.D., Costa, G.M.D.A., 2001. About the Morin transition in hematite in relation with particle size and aluminium substitution. Czech. J. Phys. 51, 663–675. https://doi.org/10.1023/A:1017697715646.
Viollier, E., Inglett, P.W., Hunter, K., Roychoudhury, A.N., Van Cappellen, P., 2000. The ferrozine method revisited: Fe(II)/Fe(III) determination in natural waters. Appl. Geochem. 15, 785–790. https://doi.org/10.1016/S0883-2927(99)00097-9.
Virkutyte, J., Sharma, V., 2014. Greener and sustainable remediation using iron nanomaterials. In: Sharma, V. (Ed.), Green Catalysts for Energy Transformation and Emission Control. American Chemical Society, Washington, D. C, pp. 1–21 ACS Symposium Series 1184, 1.
Wang, Y., Sherwood, P.M.A., 2002. Iron (III) phosphate (FePO4) by XPS. Surf. Sci. Spectra 9, 99–105. https://doi.org/10.1116/11.20030106.
Wang, Z., Fang, C., Mallavarapu, M., 2015. Characterization of iron–polyphenol complex nanoparticles synthesized by Sage (Salvia officinalis) leaves. Environmental Technology & Innovation 4, 92–97. https://doi.org/10.1016/j.eti.2015.05.004.
Wang, T., Lin, J., Chen, Z., Megharaj, M., Naidu, R., 2014a. Green synthesized iron nanoparticles by green tea and eucalyptus leaves extracts used for removal of nitrate in aqueous solution. J. Clean. Prod. 83, 413–419. https://doi.org/10.1016/j.jclepro.2014.07.006.
Wang, Z., Yu, C., Fang, C., Mallavarapu, M., 2014b. Dye removal using iron–polyphenol complex nanoparticles synthesized by plant leaves. Environmental Technology & Innovation 1, 29–34. https://doi.org/10.1016/j.eti.2014.08.003.
Weng, X., Jin, X., Lin, J., Naidu, R., Chen, Z., 2016. Removal of mixed contaminants Cr (VI) and Cu(II) by green synthesized iron based nanoparticles. Ecol. Eng. 97, 32–39. https://doi.org/10.1016/j.ecoleng.2016.08.003.